

RECORDS ADMINISTRATION
AGMW



ACC # 726374
DP-MS-73-45

MAGNETIC PROPERTIES OF TRIVALENT ACTINIDES
IN THE OCTAHEDRAL COMPOUNDS Cs_2NaMCl_6

by

M. E. Hendricks and E. R. Jones, Jr.

Department of Physics and Astronomy
University of South Carolina
Columbia, South Carolina 29208

and

J. A. Stone and D. G. Karraker

Savannah River Laboratory
E. I. du Pont de Nemours and Company
Aiken, South Carolina 29801

Proposed for publication in the
Journal of Chemical Physics

This paper was prepared in connection with work under Contract No. AT(07-2)-1 with the U. S. Atomic Energy Commission. By acceptance of this paper, the publisher and/or recipient acknowledges the U. S. Government's right to retain a non-exclusive, royalty-free license in and to any copyright covering this paper, along with the right to reproduce and to authorize others to reproduce all or part of the copyrighted paper.

SRL
RECEIVED

This document was prepared in conjunction with work accomplished under Contract No. AT(07-2)-1 with the U.S. Department of Energy.

DISCLAIMER

This report was prepared as an account of work sponsored by an agency of the United States Government. Neither the United States Government nor any agency thereof, nor any of their employees, makes any warranty, express or implied, or assumes any legal liability or responsibility for the accuracy, completeness, or usefulness of any information, apparatus, product or process disclosed, or represents that its use would not infringe privately owned rights. Reference herein to any specific commercial product, process or service by trade name, trademark, manufacturer, or otherwise does not necessarily constitute or imply its endorsement, recommendation, or favoring by the United States Government or any agency thereof. The views and opinions of authors expressed herein do not necessarily state or reflect those of the United States Government or any agency thereof.

This report has been reproduced directly from the best available copy.

Available for sale to the public, in paper, from: U.S. Department of Commerce, National Technical Information Service, 5285 Port Royal Road, Springfield, VA 22161, phone: (800) 553-6847, fax: (703) 605-6900, email: orders@ntis.fedworld.gov online ordering: <http://www.ntis.gov/ordering.htm>

Available electronically at <http://www.doe.gov/bridge>

Available for a processing fee to U.S. Department of Energy and its contractors, in paper, from: U.S. Department of Energy, Office of Scientific and Technical Information, P.O. Box 62, Oak Ridge, TN 37831-0062, phone: (865) 576-8401, fax: (865) 576-5728, email: reports@adonis.osti.gov

MAGNETIC PROPERTIES OF TRIVALENT ACTINIDES
IN THE OCTAHEDRAL COMPOUNDS $\text{Cs}_2\text{NaMCl}_6^*$

by

M. E. Hendricks[†] and E. R. Jones, Jr.Department of Physics and Astronomy
University of South Carolina
Columbia, South Carolina 29208

and

J. A. Stone and D. G. Karraker

Savannah River Laboratory
E. I. du Pont de Nemours and Company
Aiken, South Carolina 29801

ABSTRACT

The magnetic susceptibilities of U^{3+} , Np^{3+} , Pu^{3+} , Am^{3+} , Cm^{3+} , and Bk^{3+} ions in an octahedral environment were measured from 3 to about 50°K with a vibrating-sample magnetometer. Each actinide ion was in a stoichiometric compound of the cubic $\text{Cs}_2\text{NaMCl}_6$ type, except for Cm^{3+} and Bk^{3+} , which were doped into diamagnetic $\text{Cs}_2\text{NaLuCl}_6$. Curie-Weiss behavior was found for the uranium, neptunium, and plutonium compounds, with evidence for small distortions from octahedral symmetry in the uranium and plutonium compounds. The americium and berkelium samples displayed temperature-independent paramagnetism. For the curium sample, the free-ion moment was observed, but with deviations below 7.5°K that are attributed to crystal-field splitting of Cm^{3+} . The following ground levels were determined: U^{3+} , Γ_8 ; Np^{3+} , Γ_5 ;

Pu^{3+} , Γ_8 ; Am^{3+} , Γ_1 ; and Bk^{3+} , Γ_1 . In Bk^{3+} , a Γ_1 - Γ_4 separation of 85 cm^{-1} is derived. Limits on the octahedral crystal-field parameters were established from the magnetic data and from crystal-field calculations for U^{3+} and Np^{3+} , including intermediate coupling and J-mixing from the first excited states. From these parameters, the complete crystal-field splitting of each actinide ion in $\text{Cs}_2\text{NaMCl}_6$ was calculated.

INTRODUCTION

Recent studies of a new class of compounds, $\text{Cs}_2\text{NaMCl}_6$, where M is any trivalent actinide ion, have shown that the compounds are cubic; the M^{3+} ion has an octahedral environment of six chloride ligands.¹ Octahedral environments for trivalent ions have not been available previously, except with great difficulty.^{2,3} Thus, the $\text{Cs}_2\text{NaMCl}_6$ series offers one of the first opportunities to study trivalent actinides in pure compounds with a high-symmetry crystal field. Analysis of crystal-field interactions in actinide ions is difficult because of the complexity of $5f^n$ configurations, but high-symmetry fields simplify the analysis.

Detailed calculations of energies and wavefunctions for crystal-field levels of f electrons in pure J states have been presented by Lea, Leask, and Wolf⁴ (LLW) for octahedral fields. For the O_h symmetry of an octahedral environment, only two parameters, B_0^4 and B_0^6 , are required to describe the crystal-field

interaction. The ordering of the crystal-field levels is determined entirely by the ratio of these parameters, and the magnitude of the parameters determines the magnitude of the crystal-field splitting.

In this paper, the results of magnetic susceptibility measurements are given for the series of trivalent actinide ions from U^{3+} to Bk^{3+} in Cs_2NaMCl_6 for temperatures from 3 to about $50^\circ K$. Similar measurements for a rare earth compound, $Cs_2NaYbCl_6$, were reported earlier.⁵ Comparison of the results with theoretical calculations permits definition of the lowest crystal-field levels and an evaluation of limits on the crystal-field parameters. From these measurements and calculations, estimates of the importance of intermediate coupling and J-mixing are given.

EXPERIMENTAL

The cubic Cs_2NaMCl_6 compounds prepared for this study and analytical data on the samples are listed in Table I. Four of the materials ($M = U^{3+}$, Np^{3+} , Pu^{3+} , Am^{3+}) were prepared as stoichiometric compounds. Two additional actinide ions, Cm^{3+} and Bk^{3+} , because of the extremely high radioactivity of ^{244}Cm and ^{249}Bk , were doped into diamagnetic $Cs_2NaLuCl_6$. The general methods of preparation of the compounds were modeled after the procedures of Morss, Siegal, Stenger, and Edelstein.¹ Normal precautions for handling radioactive materials were exercised in each preparation.

For $\text{Cs}_2\text{NaUCl}_6$, $\text{Cs}_2\text{NaNpCl}_6$, and $\text{Cs}_2\text{NaPuCl}_6$, stoichiometric quantities of the anhydrous actinide trichloride, CsCl , and NaCl were mixed, sealed into a quartz tube, and slowly lowered (8 mm/hr) through a vertical furnace at 950°C . $\text{Cs}_2\text{NaAmCl}_6$ was prepared by dissolving stoichiometric amounts of the components in dilute HCl , evaporating the solution to dryness, vacuum-drying the solid product at 300°C , and then passing the dried crude material through the furnace as with the other compounds. Trace amounts of water and oxygen produced a slag that was removed mechanically from the solid cylinder of $\text{Cs}_2\text{NaMCl}_6$. Loss of actinide ion to the slag occasionally reduced the actinide content of the product below the theoretical formula. However, slight excesses of CsCl and NaCl did not interfere with the magnetic measurements; after magnetic measurements, each sample was dissolved and analyzed for M^{3+} (Table I).

The doped samples, $\text{Cs}_2\text{NaLu}(\text{Cm})\text{Cl}_6$ and $\text{Cs}_2\text{NaLu}(\text{Bk})\text{Cl}_6$, were prepared by dissolving a 200 mg pellet of pure $\text{Cs}_2\text{NaLuCl}_6$ in dilute HCl and then adding a small amount of Cm^{3+} or Bk^{3+} in 6M HCl , plus stoichiometric amounts of CsCl and NaCl . The same evaporation technique as for the Am^{3+} compound was followed, and fused pellets of the doped materials were obtained as with the other compounds. The initial samples of $\text{Cs}_2\text{NaLuCl}_6$ were also prepared by this procedure; the absence of magnetic impurities in the $\text{Cs}_2\text{NaLuCl}_6$ was verified by magnetometer measurements before its use as a starting material. Because of the short half-life

of ^{249}Bk (314 d), the ^{249}Cf daughter was separated by ion exchange chromatography, and the freshly purified $^{249}\text{Bk}^{3+}$ was used to prepare $\text{Cs}_2\text{NaLu}(\text{Bk})\text{Cl}_6$.

Magnetic susceptibilities were measured with a vibrating-sample magnetometer at a field of 10 000 Oe. A variable-temperature liquid-helium Dewar was employed to provide temperature control in the region 3 to 77°K. Details of the measurement technique have been given previously.⁶ For samples displaying Curie-Weiss behavior, effective magnetic moments were determined by least-squares analysis of the data.

RESULTS

Magnetic susceptibilities of the six $\text{Cs}_2\text{NaMCl}_6$ compounds were measured at temperatures 3 to 77°K (nominal). Table II summarizes the data for this series. Four of the samples ($M = \text{U}^{3+}$, Np^{3+} , Pu^{3+} , Cm^{3+}) were too weakly paramagnetic above 50°K to give accurate data.

The magnetic susceptibility of $\text{Cs}_2\text{NaUCl}_6$ (Figure 1) shows Curie-Weiss behavior in two regions below 50°K. There is an apparent break in the inverse susceptibility versus temperature plot at about 20°K, with an effective moment of $2.49 \mu_B$ below the break and $2.92 \mu_B$ above the break.

$\text{Cs}_2\text{NaNpCl}_6$ follows a single Curie-Weiss law from 3 to 50°K, as shown in Figure 2. The effective moment measured is $1.92\mu_B$.

The inverse susceptibility versus temperature plot for $\text{Cs}_2\text{NaPuCl}_6$ (Figure 3) also displays two linear regions below 50°K , with a break at about 23°K . The effective moment is $0.97 \mu_B$ below the break and $1.16 \mu_B$ above the break.

For $\text{Cs}_2\text{NaAmCl}_6$, the susceptibility was measured from 5 to 100°K . Figure 4 shows the molar susceptibility, corrected for the contribution from 50 μg of Cm^{3+} , present as an impurity. From 15 to 70°K , $\text{Cs}_2\text{NaAmCl}_6$ has temperature-independent paramagnetism, with $\chi_m = 5400 \times 10^{-6}$ emu/mole. Below 15°K , the susceptibility increases slightly, presumably due to the presence of some additional paramagnetic impurity.

Data for Cm^{3+} in $\text{Cs}_2\text{NaLuCl}_6$ are shown in Figure 5. The susceptibility exhibits Curie-Weiss behavior with an effective moment of $7.90 \mu_B$ from 7.5 to 25°K . Above 25°K , the moment appears to decrease slightly to $7.48 \mu_B$; the magnetometer signal due to Cm^{3+} was comparable to the background signal, and thus the uncertainty in the measurements above 25°K was large. Below 7.5°K , the data deviate significantly from the Curie-Weiss law.

For Bk^{3+} in $\text{Cs}_2\text{NaLuCl}_6$, the molar susceptibility (Figure 6) shows a large temperature-independent paramagnetism from 10 to 40°K , with $\chi_m = 192\,000$ emu/mole. Above 40°K , the susceptibility decreases slightly. The experimental data points are scattered because the signal from the Bk^{3+} sample was very small.

CRYSTAL-FIELD CALCULATIONS

The magnetic properties of an actinide ion in a crystal are determined by the crystal-field wavefunctions and the Boltzmann distribution of the ions among the crystal-field levels. Thus, magnetic measurements may give information on such details of the wavefunctions as the influence of intermediate coupling and J-mixing. In addition, information on the crystal-field splitting and the crystal-field parameters often can be obtained from magnetic measurements. In order to compare the experimental results with theory, crystal-field calculations applicable to $\text{Cs}_2\text{NaMCl}_6$ compounds were performed. For U^{3+} and Np^{3+} , complete intermediate-coupling wavefunctions were generated as starting points in the crystal-field calculations; J-mixing also was considered in these ions by an approximate method. Similar, but less complete, calculations were made for the other actinide ions studied.

Splitting of a $5f^n$ configuration is described by the Hamiltonian⁷

$$H = H_{\text{ES}} + H_{\text{SO}} + V \quad (1)$$

where H_{ES} is the electrostatic interaction, H_{SO} is the spin-orbit interaction, and V is the crystal-field potential. For actinide ions these interactions are not of widely different magnitudes, in contrast to those for rare earths; thus, treatment by perturbation theory may be inadequate. However, complete simultaneous diagonalization of the three Hamiltonian matrices is usually not practical because of the prohibitively large matrices required.

It is convenient to diagonalize the electrostatic and spin-orbit matrices simultaneously to obtain intermediate-coupling wavefunctions before treating the crystal-field interaction. States with the same J but different L and S are mixed by the spin-orbit interaction to give intermediate coupling wavefunctions of the form

$$|J\rangle = a_1 |L_1 S_1 J\rangle + a_2 |L_2 S_2 J\rangle + \dots \quad (2)$$

The spin-orbit interactions in actinide ions are sufficiently large that significant deviations from the nominal Russell-Saunders descriptions of the states occur. In the approximation of no J -mixing, intermediate-coupling effects are independent of the crystal field; these effects can be incorporated into the values of the Landé g_J and the factors α , β , and γ of the operator-equivalent formalism.⁸

The crystal-field potential appropriate for a site of octahedral symmetry is given by

$$V = B_0^4 [C_0^{(4)} + (5/14)^{1/2} (C_{-4}^{(4)} + C_4^{(4)})] \\ + B_0^6 [C_0^{(6)} - (7/2)^{1/2} (C_{-4}^{(6)} + C_4^{(6)})] \quad (3)$$

where B_0^4 and B_0^6 are the octahedral crystal-field parameters as defined by Wybourne,⁷ and the $C_q^{(k)}$ are tensor operators. This potential partially removes the degeneracy of a state $|J\rangle$ and splits the state into levels described by the Γ_i irreducible representations of the O_h group. The crystal-field wavefunctions have the form

$$|\Gamma_i\rangle = b_1 |J, J_z\rangle + b_2 |J, J_z+4\rangle + \dots \quad (4)$$

States of the even-electron configurations may split into Γ_1 or Γ_2 singlets, a nonmagnetic Γ_3 doublet, and Γ_4 or Γ_5 triplets; for odd-electron cases (from the O_h double group), Γ_6 or Γ_7 Kramers doublets and Γ_8 quartets may occur. Complete eigenfunctions and eigenvalues of V without J -mixing, as a function of the ratio $(B_0^6/B_0^4)(\gamma/\beta)$, have been given by LLW⁴ for all J values of interest.

The magnetic moment μ_{eff} of a level may be calculated directly from the wavefunction of the level. For the Kramers doublets and the triplets the relationship is

$$\mu_{\text{eff}} = [(S'+1)/S']^{1/2} g_J \mu_B |\langle + | J_z | + \rangle|, \quad (5)$$

where the components of a doublet are designated $|+\rangle$, $|-\rangle$, with $S' = 1/2$; a triplet has $S' = 1$, and a third component $|0\rangle$. For Γ_8 quartets with components $|+p\rangle$ and $|+r\rangle$, Bleaney⁹ gives the moment as

$$\mu_{\text{eff}} = [5(P^2 + R^2)/3]^{1/2} g_J \mu_B, \quad (6)$$

where $P = \langle +p | J_z | +p \rangle$ and $R = \langle +r | J_z | +r \rangle$. The wavefunction, and thus μ_{eff} , is independent of the crystal-field parameters for those Γ_i which occur only once in the decomposition of a state $|J\rangle$ by the octahedral crystal field.

The crystal field mixes states $|J\rangle$ with states $|J\pm 1\rangle$; in the actinides, J -mixing is known to have a significant effect on the magnetic properties of the ground state.¹⁰ The ground states of actinides are relatively well isolated, with the first excited states several thousand cm^{-1} removed. This nearest state, with

$J' = J+1$, makes the predominant contribution to J-mixing in the ground state; as a first approximation only this excited J-state will be considered in treating J-mixing in the ground state.

Using as a limited basis set the unperturbed LLW^4 wavefunctions for the states $|J\rangle$ and $|J+1\rangle$, the following 2×2 matrix¹¹ can be diagonalized:

$$\begin{pmatrix} \langle J, \Gamma_i | V | J, \Gamma_i \rangle & \langle J, \Gamma_i | V | J+1, \Gamma_i \rangle \\ \langle J+1, \Gamma_i | V | J, \Gamma_i \rangle & E + \langle J+1, \Gamma_i | V | J+1, \Gamma_i \rangle \end{pmatrix} \quad (7)$$

where E is the energy of the first excited state. This procedure gives a J-mixed wavefunction,

$$|\Gamma'_i\rangle = c_1 |J, \Gamma_i\rangle + c_2 |J+1, \Gamma_i\rangle \quad (8)$$

with $|c_2|^2 \ll 1$, from which the moment may be calculated. Cross-terms such as $c_1 c_2 \langle J, \Gamma_i | L_z + 2S_z | J+1, \Gamma_i \rangle$ are given by the formulas of Elliott and Stevens,¹² using intermediate-coupling values for the Landé g-factors.

Of the compounds considered in this study, those containing U^{3+} and Np^{3+} have the most simple electronic configurations; for those compounds detailed calculations of μ_{eff} were performed as a function of the crystal-field strength (and thus of the extent of J-mixing). Intermediate-coupling wavefunctions were generated by simultaneously diagonalizing the electrostatic and spin-orbit Hamiltonian matrices. Values for the F_2 Slater integral and the spin-orbit coupling constant ζ were taken from the work of Carnall and Wybourne,¹³ with F_4 and F_6 obtained from the approximation of hydrogenic ratios.¹⁴ From these wavefunctions g_J and the operator-equivalent factors, α , β , and γ , were calculated in intermediate

coupling for the ground state and first excited state of U^{3+} and Np^{3+} (Table III). Matrix elements of V were obtained by the tensor-operator method,¹⁴ using tabulated values of reduced matrix elements,¹⁵ 3-J, and 6-J symbols.¹⁶

An order-of-magnitude estimate of crystal-field parameters for the Cs_2NaMCl_6 compounds may be obtained from a comparison of crystal-field parameters reported for similar octahedral chloride lattices. Table IV gives values of B_0^4 and B_0^6 from absorption spectra or magnetic studies for several MCl_6^{n-} systems. These data indicate that the B_0^6/B_0^4 ratio lies within 0 to +1, and that B_0^4 may be between 200 to 8000 cm^{-1} . This information permits realistic limits on the crystal-field parameters to be set for computational purposes. In this work, J-mixed crystal-field wavefunctions and values of μ_{eff} were calculated by systematically varying B_0^4 from 0 to +20 000 cm^{-1} , and varying the ratio B_0^6/B_0^4 from 0 to +1.0, for U^{3+} and Np^{3+} . The results of these calculations and comparison with the experimental measurements are described in the following section.

SUSCEPTIBILITY MEASUREMENTS

Cs_2NaUCl_6

The U^{3+} ion in Cs_2NaUCl_6 has a $5f^3$ configuration with the ground state nominally $^4I_{9/2}$. However, the large spin-orbit interaction mixes significant amounts of other terms with $J = 9/2$ into the ground state.¹⁷ Using electrostatic¹⁵ and spin-orbit¹⁸

interaction matrices for f^3 , with $\zeta = 1666 \text{ cm}^{-1}$ and $F_2 = 196 \text{ cm}^{-1}$, the intermediate-coupling wavefunctions for the $J = 9/2$ ground state and the $J = 11/2$ first-excited state of U^{3+} were calculated. The lowest-energy eigenfunctions of the 7×7 (for $J = 9/2$) and 5×5 (for $J = 11/2$) matrices are given in Table V. These wavefunctions were used to calculate intermediate-coupling values of g_J (given in Table III) and as basis functions for J-mixing calculations. For the ground state this value of g_J leads to a free-ion moment of $3.69 \mu_B$ for U^{3+} .

The LLW^4 crystal-field calculations for a $J = 9/2$ state in octahedral symmetry show that the ground level may be either a Γ_8 quartet or a Γ_6 doublet, depending on the value of B_0^6/B_0^4 . As a first approximation (intermediate coupling without J-mixing), magnetic moments calculated from the LLW^4 wavefunctions can be compared with the experimental results for Cs_2NaUCl_6 . For the Γ_8 level, the calculation gives $2.81 \mu_B \leq \mu_{\text{eff}} \leq 2.84 \mu_B$ for B_0^6/B_0^4 ratios between 0 and +1; for the Γ_6 level the calculated moment is $\mu_{\text{eff}} = 2.36 \mu_B$ for all B_0^6/B_0^4 ratios. The magnetic susceptibility data for Cs_2NaUCl_6 (Figure 1) yield an experimental moment below 20°K that is near the calculated value for the Γ_6 level, and above 25°K , near the calculated value for the Γ_8 level. However, in both cases the calculated moments are outside the experimental error limits.

The effects of J-mixing by the $J = 11/2$ state¹⁹ at $E = 4185$ cm^{-1} in U^{3+} were taken into account in more extensive calculations. In Figure 7, the calculated moments are shown as a function of B_0^4 . For the Γ_8 level, results for several values of B_0^6/B_0^4 are shown; for the Γ_6 level, the moments are independent of this ratio. J-mixing brings the theoretical moments for the Γ_8 level into agreement with the experimental moment above 25°K . For a given value of B_0^6/B_0^4 , a range of B_0^4 values is compatible with the experimental results, but this range becomes narrower as B_0^6/B_0^4 increases. The results for the Γ_8 level are consistent with B_0^4 in the range 200 to 8000 cm^{-1} (Table IV). J-mixing causes the calculated moment for the Γ_6 level to diverge from the low-temperature (below 20°K) experimental moment.

This analysis indicates that the lowest crystal-field level of $\text{Cs}_2\text{NaUCl}_6$ is a Γ_8 level slightly distorted from octahedral symmetry. Any distortion will split the Γ_8 quartet into two Kramers doublets, each with a smaller moment than the Γ_8 level. Thus, the lower moment observed below 20°K can be attributed to the unequal thermal population of the two doublets; above 25°K , the populations are essentially equal, and the Γ_8 moment is observed. An alternative interpretation places the Γ_6 level lowest, with an undistorted Γ_8 level about 10 cm^{-1} higher; however, this explanation appears unlikely because of the poor agreement of the data with the calculated Γ_6 moment.

Cs₂NaNpCl₆

The Np³⁺ ion has a 5f⁴ configuration and a nominal ⁵I₄ ground state in Cs₂NaNpCl₆. Intermediate-coupling wavefunctions for the J = 4 ground state and the J = 5 first-excited state of Np³⁺ were calculated by the same method as for U³⁺. For Np³⁺, the electrostatic¹⁵ and spin-orbit²⁰ interaction matrices for f⁴ were used, with $\zeta = 2070 \text{ cm}^{-1}$ and $F_2 = 225 \text{ cm}^{-1}$. The lowest-energy eigenfunctions of the 19 x 19 (for J = 4) and 14 x 14 (for J = 5) matrices are given in Table VI, from which the intermediate-coupling values of g_J were calculated (Table III). The free-ion moment of Np³⁺ is 2.89 μ_B.

For a J = 4 state in octahedral symmetry, the LLW⁴ crystal-field calculations show that the ground level may be either a Γ₁ singlet or a Γ₅ triplet, depending on the value of B₀⁶/B₀⁴. The Curie-Weiss behavior of Cs₂NaNpCl₆ down to 3°K rules out the possibility of a Γ₁ ground state, which would exhibit only temperature-independent paramagnetism. Thus, the ground level of Np³⁺ in Cs₂NaNpCl₆ is expected to be a Γ₅ triplet. The magnetic moment of the Γ₅ level, calculated from the intermediate-coupling value of g_J and the LLW⁴ wavefunction, is 2.29 μ_B; this value exceeds the experimental moment of Cs₂NaNpCl₆ by about 20%.

A better approximation allows for J-mixing by the J = 5 state¹⁹ at 3768 cm⁻¹ in Np³⁺. Results of this calculation are shown in Figure 8, where the calculated moments are given as a

function of B_0^4 for several values of B_0^6/B_0^4 . These may be compared with the experimental moment for $\text{Cs}_2\text{NaNpCl}_6$ from the magnetic susceptibility data of Figure 2. J-mixing reduces the calculated moment and tends to bring it into agreement with the experimental moment. Fairly large values of B_0^6/B_0^4 are required to give agreement between experimental and calculated moments for values of B_0^4 less than 8000 cm^{-1} . With the large matrices used, these calculations may be subject to considerable uncertainties; their chief value is in demonstrating the correct trend of the effective magnetic moment with J-mixing.

Because the experimental data for $\text{Cs}_2\text{NaNpCl}_6$ are in qualitative agreement with the theoretical treatment, the lowest crystal-field level is assigned as a Γ_5 triplet. No evidence for a distortion from octahedral symmetry is found in the magnetic data. The experimental moment for Np^{3+} in $\text{Cs}_2\text{NaNpCl}_6$, $1.92 \mu_B$, is in excellent agreement with moments measured for isoelectronic Pu^{4+} in octahedral PuCl_6^{2-} complexes.²¹

$\text{Cs}_2\text{NaPuCl}_6$

The ground state of Pu^{3+} ($5f^5$), nominally ${}^6\text{H}_{5/2}$, has been shown to contain only 66% ${}^6\text{H}_{5/2}$ character because of strong intermediate coupling.¹¹ In an octahedral crystal field the $J = 5/2$ state splits into two levels, a Γ_7 doublet and a Γ_8 quartet. An interesting consequence of the strong intermediate coupling is a sign change in the fourth-order operator-equivalent factor β for Pu^{3+} , and thus the order of the two crystal-field

levels is inverted from that of the Russell-Saunders case.¹¹ The value of g_J also is markedly different from the Russell-Saunders value of $g_J = 2/7 = 0.286$; from the 28-term intermediate-coupling wavefunction¹¹ of Pu^{3+} , $g_J = 0.421$. This value gives a free-ion moment of $1.25 \mu_B$ for Pu^{3+} .

From the LLW⁴ calculations, with negative β for Pu^{3+} , the ground level is expected to be the Γ_8 quartet in octahedral symmetry. The effective moments of the Γ_7 and Γ_8 levels, calculated from the LLW⁴ wavefunctions, are $0.61 \mu_B$ for the Γ_7 level and $1.03 \mu_B$ for the Γ_8 level. The experimental moments from Figure 3, $0.97 \mu_B$ (3 to 21°K) and $1.16 \mu_B$ (25 to 50°K), are consistent with a Γ_8 ground level in $\text{Cs}_2\text{NaPuCl}_6$ and with the theoretical prediction of a negative value of β . One interpretation of the data assigns the low-temperature moment to the Γ_8 level, with the free-ion moment observed at higher temperatures; this would require a very small Γ_8 - Γ_7 separation, $\sim 10 \text{ cm}^{-1}$. The experimental and calculated moments are in excellent agreement, perhaps fortuitously so, because J-mixing is not considered. Alternatively, the break in the susceptibility data may signify a small distortion of the Γ_8 level, just as for $\text{Cs}_2\text{NaUCl}_6$, with the full moment of the Γ_8 level being observed only above 25°K. Although agreement with the calculated moment is not as good in this case, it is nevertheless considered the more likely interpretation, because the effects of J-mixing are known to be important in Pu^{3+} .^{10,11}

Cs₂NaAmCl₆

Intermediate-coupling effects in the 5f⁶ Am³⁺ ion are severe, with the J = 0 ground state having only 47% of its nominal ⁷F₀ the character.¹³ Systems with J = 0 have no first-order Zeeman effect, so that the observed temperature-independent paramagnetic susceptibility of Cs₂NaAmCl₆ must arise from the second-order Zeeman effect. This interaction is between the singlet ground state of Am³⁺ and the J = 1 triplet state²² at 2720 cm⁻¹, neither of which is split by an octahedral field.

The standard treatment of second-order Zeeman effect between states with ΔJ = ±1, for a free ion in Russell-Saunders coupling, gives²³

$$\chi_{\text{TIP}} = \frac{N\mu_B^2}{6(2J+1)} \left[\frac{F(J+1)}{\Delta E_{J+1,J}} - \frac{F(J)}{\Delta E_{J,J-1}} \right], \quad (9)$$

where N is Avagadro's number, and

$$F(J) = [(S+L+1)^2 - J^2][J^2 - (S-L)^2]/J. \quad (10)$$

Using the measured susceptibility of Cs₂NaAmCl₆, (5400 ± 400) × 10⁻⁶ emu/mole, and ΔE_{1,0} = 2720 cm⁻¹, an experimental value of F(1) may be obtained from Equation 9. This procedure gives F(1) = 338 ± 25, compared with the value of 48 calculated from Equation 10 for a pure ⁷F₁ state. The large discrepancy apparently cannot be explained by intermediate-coupling effects because these would tend to reduce further the calculated F(1). The presence of J-mixing in the ⁷F term, for which Equation 9 does not hold, must be considered as a possible explanation for the apparently anomalous magnitude of χ_{TIP} in Cs₂NaAmCl₆.

Cm^{3+} in $\text{Cs}_2\text{NaLuCl}_6$

The $5f^7$ configuration of Cm^{3+} corresponds to a half-filled shell, with an $^8\text{S}_{7/2}$ ground state in Russell-Saunders coupling. Pure S terms do not interact with the crystal field (α , β , and γ are zero) and have $g_J = 2.000$. However, Cm^{3+} is known to have considerable intermediate coupling²⁴; evaluation of the 50-term wavefunction shows that the ground state has only 79% $^8\text{S}_{7/2}$ character. Edelstein and Easley²⁴ have given the values of g_J , α , β , and γ for Cm^{3+} shown in Table III. Crystal-field splitting of Cm^{3+} in various cubic environments²⁵ is quite large (20 to 40 cm^{-1}) compared with the corresponding $4f^7$ ion, Gd^{3+} , for which intermediate-coupling effects are smaller. From these considerations, the free-ion moment of Cm^{3+} , $7.64 \mu_B$, is expected at all except the lowest temperatures, where effects of the crystal-field splitting may be observed. J-mixing should be insignificant for the ground state of Cm^{3+} because it is well isolated from the first-excited state²⁶ at $\sim 17\,000 \text{ cm}^{-1}$.

Susceptibility data for Cm^{3+} in $\text{Cs}_2\text{NaLuCl}_6$ (Figure 5) are in reasonably good agreement with the free-ion moment, down to 7.5°K . Below 7.5°K , the data deviate from the free-ion moment, suggesting a crystal-field splitting of about 5 to 10 cm^{-1} . A splitting of this magnitude for Cm^{3+} in an octahedral chloride lattice is consistent with Cm^{3+} splittings in other lattices. In octahedral symmetry, a $J = 7/2$ state splits into a Γ_6 , a Γ_7 , and a Γ_8 level;

however, because these levels are closely spaced for Cm^{3+} in $\text{Cs}_2\text{NaLuCl}_6$, the magnetic data are not sufficient to determine their order and spacings. Experiments with Cm^{3+} at the dopant level were facilitated by the large effective moment, which gave an adequate signal even with the small mass of curium used.

Bk^{3+} in $\text{Cs}_2\text{NaLuCl}_6$

The Bk^{3+} ion ($5f^8$) has the Russell-Saunders ground state 7F_6 , but intermediate coupling and J-mixing are expected to be important. Intermediate-coupling wavefunctions for Bk^{3+} have not been published, and thus splitting factors like those in Table III are not yet available²⁷ for Bk^{3+} . As a rough approximation, the corresponding quantities for Tb^{3+} ($4f^8$) have been used for Bk^{3+} , assuming no irregular behavior such as the sign change in β that occurs for Pu^{3+} .

Crystal-field splitting of a $J = 6$ state in octahedral symmetry, from the LLW⁴ calculations, gives either a Γ_1 singlet or a Γ_2 singlet as the ground level, depending on the value of B_0^6/B_0^4 . Either singlet level would have only a second-order Zeeman effect, consistent with the temperature-independent paramagnetism observed for Bk^{3+} in $\text{Cs}_2\text{NaLuCl}_6$. The Γ_1 singlet is assigned as the ground level of Bk^{3+} for reasons given in the following section; only the Γ_1 level is compatible with B_0^6/B_0^4 values between 0 and +1. To account for the extremely large value of χ_{TIP} , a nearby level connected to the Γ_1 level by a nonzero matrix element is required. The LLW⁴ wavefunctions for $J = 6$ show that the Γ_1 level has a nonzero matrix element only with a Γ_4

level, with $|\langle \Gamma_1 | J_z | \Gamma_4 \rangle|^2 = 14$, and that these two levels are adjacent in energy.

For this case the susceptibility is given by

$$\chi_{\text{TIP}} = \frac{2N\mu_B^2}{hc} \left[\frac{|\langle \Gamma_1 | J_z | \Gamma_4 \rangle|^2}{\Delta E_{4,1}} \right] g_J^2 \quad (11)$$

Using the Russell-Saunders $g_J = 1.5$ and the experimental χ_{TIP} , the energy separation of the Γ_1 and Γ_4 levels is calculated as $\Delta E_{4,1} = 85 \text{ cm}^{-1}$. A splitting of this magnitude is not inconsistent with the data (Figure 6), which show no magnetic levels populated below about 50 cm^{-1} ; however, the calculated separation is subject to the uncertainties of both the experimental susceptibility ($\sim 15\%$) and the g_J value.

DISCUSSION

For most of the $\text{Cs}_2\text{NaMCl}_6$ compounds the lowest crystal-field level can be identified from the susceptibility data, but little direct information is gained on crystal-field splittings and crystal-field parameters for the compounds. Only in the case of Bk^{3+} is an energy separation determined from the data. However, from the crystal-field classifications of the ground levels, particularly of U^{3+} and Np^{3+} , limits may be set on the B_0^6/B_0^4 ratio by using LLW⁴ theory. These limits, combined with the Bk^{3+} Γ_1 - Γ_4 separation, lead to an evaluation of limits on the B_0^4 parameter. Thus, two limiting sets of crystal-field parameters are generated that may be applied to calculate complete crystal-field splittings of each actinide ion in the octahedral $\text{Cs}_2\text{NaMCl}_6$ environment.

For U^{3+} in octahedral symmetry, the only possibilities for the lowest level are the Γ_6 and $\Gamma_8^{(2)}$ crystal-field levels, as shown by the LLW⁴ calculations for $J = 9/2$. The value of B_0^6/B_0^4 at the Γ_6 - $\Gamma_8^{(2)}$ crossover point is

$$B_0^6/B_0^4 = (1/105)(\beta/\gamma) \quad \text{for } E(\Gamma_6) = E(\Gamma_8^{(2)}). \quad (12)$$

From Table III, β/γ for U^{3+} is +7.09, and from the experimental observation that the ground level is the $\Gamma_8^{(2)}$ level, a lower limit on B_0^6/B_0^4 may be set:

$$[U^{3+}] \quad (B_0^6/B_0^4) \geq +0.0676 \quad (13)$$

Similarly, for Np^{3+} in octahedral symmetry the LLW⁴ calculations for $J = 4$ show that the Γ_1 and Γ_5 levels are the only possibilities for the lowest level. The Γ_1 - Γ_5 crossover point is given by

$$B_0^6/B_0^4 = (3/35)(\beta/\gamma) \quad \text{for } E(\Gamma_1) = E(\Gamma_5). \quad (14)$$

The magnetic susceptibility data for Np^{3+} place the Γ_5 level lowest; with $\beta/\gamma = +7.18$ (Table III), Equation 14 permits the following limits to be set:

$$[Np^{3+}] \quad 0 \leq (B_0^6/B_0^4) \leq +0.616. \quad (15)$$

To proceed further requires a relationship among the values of B_0^6/B_0^4 for different members of the Cs_2NaMCl_6 series. The B_0^6/B_0^4 ratio is expected to change slowly from $M = U^{3+}$ to $M = Bk^{3+}$, because the site symmetry of the actinide ion is the same for each member, the size of the unit cell is approximately the same in each case, and the ligands are the same in every case. As a first approximation, B_0^6/B_0^4 has been assumed constant across the series. This assumption, together with the experimental data, permits limits to be set for both the B_0^6/B_0^4 ratio and the B_0^4 crystal-field

parameter. Combining the limits from U^{3+} and Np^{3+} data gives

$$[Cs_2NaMCl_6] \quad +0.0676 \leq (B_0^6/B_0^4) \leq +0.616. \quad (16)$$

Then, limits on B_0^4 may be established from the Bk^{3+} data.

For Bk^{3+} , Equation 16 may be used to identify the ground level. The LLW⁴ calculations for $J = 6$ show a crossover of Γ_1 and Γ_2 levels, the only possibilities for the lowest level of Bk^{3+} in octahedral symmetry. At the crossover point the value of B_0^6/B_0^4 is given by

$$B_0^6/B_0^4 = -(2/105)(\beta/\gamma) \quad \text{for } E(\Gamma_1) = E(\Gamma_2). \quad (17)$$

Although a value of β/γ for Bk^{3+} is not available, the value for Tb^{3+} $(-109.20)^4$ may be substituted in a rough approximation, giving the following limits for the Γ_1 level:

$$[Bk^{3+}] \quad 0 \leq (B_0^6/B_0^4) \leq +2.08 \quad (18)$$

This range of values encompasses the limits given in Equation 16 for the entire Cs_2NaMCl_6 series and is the justification for assigning the lowest level of Bk^{3+} in $Cs_2NaLuCl_6$ as the Γ_1 level. The Γ_2 level, with $(B_0^6/B_0^4) \geq +2.08$, is far beyond the range of Equation 16 and is thus excluded.

The Γ_1 - Γ_4 separation in Bk^{3+} , which was determined from the experimental data, also may be expressed in terms of B_0^4 and B_0^6/B_0^4 ; from the LLW⁴ eigenvalues the separation is given by

$$\Delta E_{4,1} = B_0^4 [225\beta - 11340\gamma(B_0^6/B_0^4)]. \quad (19)$$

Again using Tb^{3+} values⁸ for β and γ , with $\Delta E_{4,1} = 85 \text{ cm}^{-1}$, and substituting the limiting values of B_0^6/B_0^4 from Equation 16, lead to a rather narrow range of values for B_0^4 :

$$[Cs_2NaMCl_6] \quad 3015 \geq B_0^4 \geq 2420 \text{ cm}^{-1} \quad (20)$$

Thus, the assumption of constant crystal-field parameters within the $\text{Cs}_2\text{NaMCl}_6$ series, and the other approximations introduced, give two limiting sets of parameters,

$$\text{Case A: } B_0^4 = 2420 \text{ cm}^{-1}; \quad B_0^6 = 1490 \text{ cm}^{-1}; \quad B_0^6/B_0^4 = 0.616$$

$$\text{Case B: } B_0^4 = 3015 \text{ cm}^{-1}; \quad B_0^6 = 204 \text{ cm}^{-1}; \quad B_0^6/B_0^4 = 0.0676 .$$

As a check on the consistency of this analysis, the complete ground-state crystal-field splitting of each actinide ion in $\text{Cs}_2\text{NaMCl}_6$ was calculated with these parameters, using the LLW⁴ solutions of Equation 3. Figure 9 shows the calculated crystal-field levels of U^{3+} , Np^{3+} , Pu^{3+} , Cm^{3+} , and Bk^{3+} for the two limiting cases; of course, Am^{3+} , with $J = 0$, is not split.

The calculations for each ion may be compared with experimental information. Large crystal-field splittings were calculated for $\text{Cs}_2\text{NaUCl}_6$ and $\text{Cs}_2\text{NaNpCl}_6$. In U^{3+} , the overall splitting is between 385 cm^{-1} (Case B) and 875 cm^{-1} (Case A), and in Np^{3+} between 446 and 811 cm^{-1} . With such large splittings, it is likely that the lowest crystal-field level will be isolated, in agreement with the experimental data for $\text{Cs}_2\text{NaUCl}_6$ and $\text{Cs}_2\text{NaNpCl}_6$. Considerably smaller splitting is calculated for the Γ_8 - Γ_7 separation in $\text{Cs}_2\text{NaPuCl}_6$, 38 to 47 cm^{-1} , depending only on the value of B_0^4 . A splitting of this magnitude is too large to account for the break in the Pu^{3+} susceptibility data at about 23°K , and supports the interpretation of a distorted Γ_8 ground level. For $\text{Cs}_2\text{NaCmCl}_6$, overall crystal-field splitting of 13 to 15 cm^{-1} is calculated;

the experimental departure from the free-ion moment at low temperatures is consistent with a splitting of this magnitude for Cm^{3+} . The six crystal-field levels of Bk^{3+} span 584 cm^{-1} (Case A) to 672 cm^{-1} (Case B).

These calculated splittings may be regarded as first approximations derived from the magnetic susceptibility data, and are useful in demonstrating differences in behavior from element to element. The relative splittings of each actinide ion in the octahedral Cs_2NaMCl_6 environment may be reasonably accurate. However, all the limitations pointed out by LLW⁴ for their eigenvalue expressions apply to the present calculations. Especially serious is the neglect of J-mixing, which has been shown to produce significant alterations in crystal-field splittings and magnetic properties in some cases (for example, in $PaCl_4$).²⁸ Analysis of the susceptibility data with respect to J-mixing and intermediate coupling was discussed earlier; intermediate coupling in the actinides is well known as a large and significant effect, but one that is fairly simple to take into account. On the other hand, J-mixing is less well understood and considerably more difficult to calculate. With data now available for the actinides, however, it is becoming increasingly apparent that J-mixing is an important effect that must be considered in any detailed analysis of actinide ions in crystals.

REFERENCES

*The information contained in this article was developed during the course of work under Contract AT(07-2)-1 with the U. S. Atomic Energy Commission.

†AEC Special Fellow in Nuclear Science and Engineering.

Present address: Wofford College, Spartanburg, S. C. 29301.

1. L. R. Morss, M. Siegal, L. Stenger, and N. Edelstein, *Inorg. Chem.* **9**, 1771 (1970).
2. D. Brown, *Halides of the Lanthanides and Actinides* (Wiley, London, 1968), pp. 158-9.
3. R. E. Stevens, *J. Inorg. Nucl. Chem.* **27**, 1873 (1965).
4. K. R. Lea, M. J. M. Leask, and W. P. Wolf, *J. Phys. Chem. Solids* **23**, 1381 (1962).
5. D. G. Karraker, *J. Chem. Phys.* **55**, 1084 (1971).
6. J. A. Stone and E. R. Jones, Jr., *J. Chem. Phys.* **54**, 1713 (1971).
7. B. G. Wybourne, *Spectroscopic Properties of Rare Earths* (Interscience, New York, 1965).
8. K. W. H. Stevens, *Proc. Phys. Soc. (London)* **A65**, 209 (1952).
9. B. Bleaney, *Proc. Phys. Soc. (London)* **73**, 939 (1959).
10. D. J. Lam and S. K. Chan, *Phys. Rev. B* **6**, 307 (1972).
11. N. Edelstein, H. F. Mollet, W. C. Easley, and R. J. Mehlhorn, *J. Chem. Phys.* **51**, 3281 (1969).
12. R. J. Elliott and K. W. H. Stevens, *Proc. Roy. Soc. (London)* **A218**, 553 (1953).
13. W. T. Carnall and B. G. Wybourne, *J. Chem. Phys.* **40**, 3428 (1964).

14. B. R. Judd, *Operator Techniques in Atomic Spectroscopy* (McGraw-Hill, New York, 1963).
15. C. W. Nielson and G. F. Koster, *Spectroscopic Coefficients for p^n , d^n , and f^n Configurations* (The M.I.T. Press, Cambridge, Massachusetts, 1963).
16. M. Rotenberg, R. Bivins, N. Metropolis, and J. K. Wooten, *The 3-J and 6-J Symbols* (The Technology Press, Cambridge, Massachusetts, 1959).
17. L. P. Varga, M. J. Reisfeld, and L. B. Asprey, *J. Chem. Phys.* **53**, 250 (1970).
18. B. R. Judd and R. Loudon, *Proc. Roy. Soc. (London)* **A251**, 127 (1959).
19. N. Edelstein (private communication).
20. M. H. Crozier and W. A. Runciman, *J. Chem. Phys.* **35**, 1392 (1961).
21. D. G. Karraker, *Inorg. Chem.* **10**, 1564 (1971).
22. J. G. Conway, *J. Chem. Phys.* **40**, 2504 (1964).
23. J. H. Van Vleck, *The Theory of Electric and Magnetic Susceptibilities* (Oxford University Press, London, 1932).
24. N. Edelstein and W. Easley, *J. Chem. Phys.* **48**, 2110 (1968).
25. W. Kolbe, N. Edelstein, C. B. Finch, and M. M. Abraham, *J. Chem. Phys.* **56**, 5432 (1972).
26. J. B. Gruber, W. R. Cochran, J. G. Conway, and A. T. Nicol, *J. Chem. Phys.* **45**, 1423 (1966).
27. W. T. Carnall, S. Fried, F. Wagner, Jr., R. F. Barnes, R. K. Sjoblom, and P. R. Fields, *Inorg. Nucl. Chem. Lett* **8**, 773 (1972).
28. M. E. Hendricks, E. R. Jones, Jr., J. A. Stone, and D. G. Karraker, *J. Chem. Phys.* **55**, 2993 (1971).

TABLE I. Analytical data for the samples studied.

Sample	Actinide Isotope	Weight (mg)	Actinide Content (%)		Analytical Method
			Calculated	Found	
$\text{Cs}_2\text{NaUCl}_6$	238	339.57	32.17	25.8 \pm 0.1	<i>a</i>
$\text{Cs}_2\text{NaNpCl}_6$	237	315.04	32.08	33.2 \pm 1.0	<i>b</i>
$\text{Cs}_2\text{NaPuCl}_6$	239	327.24	32.27	30.8 \pm 1.0	<i>b, c</i>
$\text{Cs}_2\text{NaAmCl}_6^d$	243	191.57	32.45	15.7 \pm 0.5 ^e	<i>b</i>
$\text{Cs}_2\text{NaLu(Cm)Cl}_6$	244	3.22 ^f	-----	-----	<i>b, c</i>
$\text{Cs}_2\text{NaLu(Bk)Cl}_6^g$	249	0.624 ^f	-----	-----	<i>b, c, h</i>

a. Chemical analysis.

b. Alpha counting, pulse-height analysis.

c. Isotopic analysis by mass spectrometry.

d. Sample contained 50 μg Cm^{3+} impurity.

e. Balance of sample was a mixture of CsCl and NaCl .

f. Weight of actinide doped into $\text{Cs}_2\text{NaLuCl}_6$.

g. Sample contained 4 μg Cf^{3+} impurity at the time of the magnetic measurements.

h. Scintillation gamma counting.

TABLE II. Magnetic data for octahedral actinide(III) chlorides.

Compound	T (°K)	μ_{eff} (μ_B)	C^a [(emu-°K)/mole]	θ^a (°K)	χ_{TIP}^b (10^{-6} emu/mole)
Cs ₂ NaUCl ₆	4 to 20	2.49 ±0.06	0.778	0.53	-----
	25 to 50	2.92 ±0.06	1.066	9.6	-----
Cs ₂ NaNpCl ₆	3 to 50	1.92 ±0.05	0.46	0.47	-----
Cs ₂ NaPuCl ₆	3 to 21	0.97 ±0.05	0.117	1.3	-----
	25 to 50	1.16 ±0.08	0.167	12.4	-----
Cs ₂ NaAmCl ₆	15 to 70	-----	-----	-----	5400 ±400
Cs ₂ NaCmCl ₆ ^c	7.5 to 25	7.90 ±0.10	7.81	3.87	-----
	25 to 45	7.48 ±0.50	6.99	1.15	-----
Cs ₂ NaBkCl ₆ ^c	10 to 40	-----	-----	-----	192 000 ±30 000

a. Paramagnetic constants from Curie-Weiss law $\chi = C/(T+\theta)$.

b. Temperature-independent paramagnetic susceptibility.

c. Doped into Cs₂NaLuCl₆.

TABLE III. Calculated Landé g factors and operator equivalent factors, with intermediate coupling.

Ion	J^a	g_J	$10^3 \alpha$	$10^4 \beta$	$10^6 \gamma$
U^{3+}	9/2	0.7434	-5.72	-2.584	-36.45
U^{3+}	$11/2^b$	0.9715	-4.62	-0.893	-2.66
Np^{3+}	4	0.6457	7.17	4.235	58.94
Np^{3+}	5^b	0.9133	5.23	1.645	-2.67
Pu^{3+c}	5/2	0.4211	44.77	-3.476	0
Cm^{3+d}	7/2	1.9261	-1.397	0.2109	-0.8933

a. For ground state of the ion, except as noted.

b. First excited state.

c. Reference 11.

d. Reference 24.

TABLE IV. Crystal-field parameters of actinide and rare earth ions in octahedral chloride lattices.

Ion	B_0^4 (cm^{-1})	B_0^6 (cm^{-1})	B_0^6/B_0^4	Reference
PaCl_6^{2-}	7104	670	+0.095	<i>c</i>
UCl_6^{2-}	7296	904	+0.124	<i>d</i>
NpCl_6^{2-}	4160	2400	+0.577	<i>e</i>
PuCl_6^{2-a}	424	256	+0.604	21
NdCl_6^{3-}	2256	1195	+0.530	<i>f</i>
$\text{YbCl}_6^{3-a,b}$	285	37	+0.130	5

a. Derived from magnetic susceptibility data; all other values are from optical spectroscopy.

b. Average of maximum and minimum values for $\text{Cs}_2\text{NaYbCl}_6$.

c. J. D. Axe, H. J. Stapleton, and C. D. Jeffries, Phys. Rev. *121*, 1630 (1961).

d. R. A. Satten, C. L. Schreiber, and E. Y. Wong, J. Chem. Phys. *42*, 162 (1965).

e. E. R. Menzel and J. B. Gruber, J. Chem. Phys. *54*, 3857 (1971).

f. J. B. Gruber, E. R. Menzel, and J. L. Ryan, J. Chem. Phys. *51*, 3816 (1969).

TABLE V. Intermediate-coupling wavefunctions of the ground state ($J = 9/2$) and the first-excited state ($J = 11/2$) of U^{3+} .

Term	J = 9/2 State		J = 11/2 State	
	Coeff.	Coeff. ² (%)	Coeff.	Coeff. ² (%)
⁴ F	0.0193	0.037		
⁴ G	0.0306	0.094	0.0346	0.120
⁴ I	0.9592	92.012	0.9741	94.886
² G1	-0.0578	0.334		
² G2	0.0511	0.261		
² H1	0.0986	0.973	0.0834	0.696
² H2	-0.2508	6.289	-0.2046	4.186
² I			-0.0337	0.113

TABLE VI. Intermediate-coupling wavefunctions of the ground state ($J = 4$) and the first-excited state ($J = 5$) of Np^{3+} .

Term	J = 4 State		J = 5 State	
	Coeff.	Coeff. ² (%)	Coeff.	Coeff. ² (%)
⁵ D	-0.0061	0.004		
⁵ F	0.0208	0.043	0.0150	0.023
⁵ G	-0.0384	0.147	-0.0442	0.195
⁵ I	0.8969	80.445	0.9507	90.390
³ F1	-0.0113	0.013		
³ F2	0.0156	0.024		
³ F3	-0.0156	0.024		
³ F4	0.0312	0.097		
³ G1	0.0225	0.051	0.0083	0.007
³ G2	0.0877	0.768	0.0557	0.310
³ G3	-0.0582	0.338	-0.0338	0.114
³ H1	0.1918	3.680	0.1266	1.602
³ H2	-0.0268	0.072	0.0062	0.004
³ H3	0.1970	3.883	0.1494	2.232
³ H4	-0.3046	9.278	-0.2169	4.704
³ I1			-0.0431	0.186
³ I2			-0.0446	0.199
¹ G1	0.0528	0.279		
¹ G2	-0.0263	0.069		
¹ G3	0.0263	0.069		
¹ G4	0.0845	0.715		
¹ H1			0.0173	0.030
¹ H2			0.0060	0.004

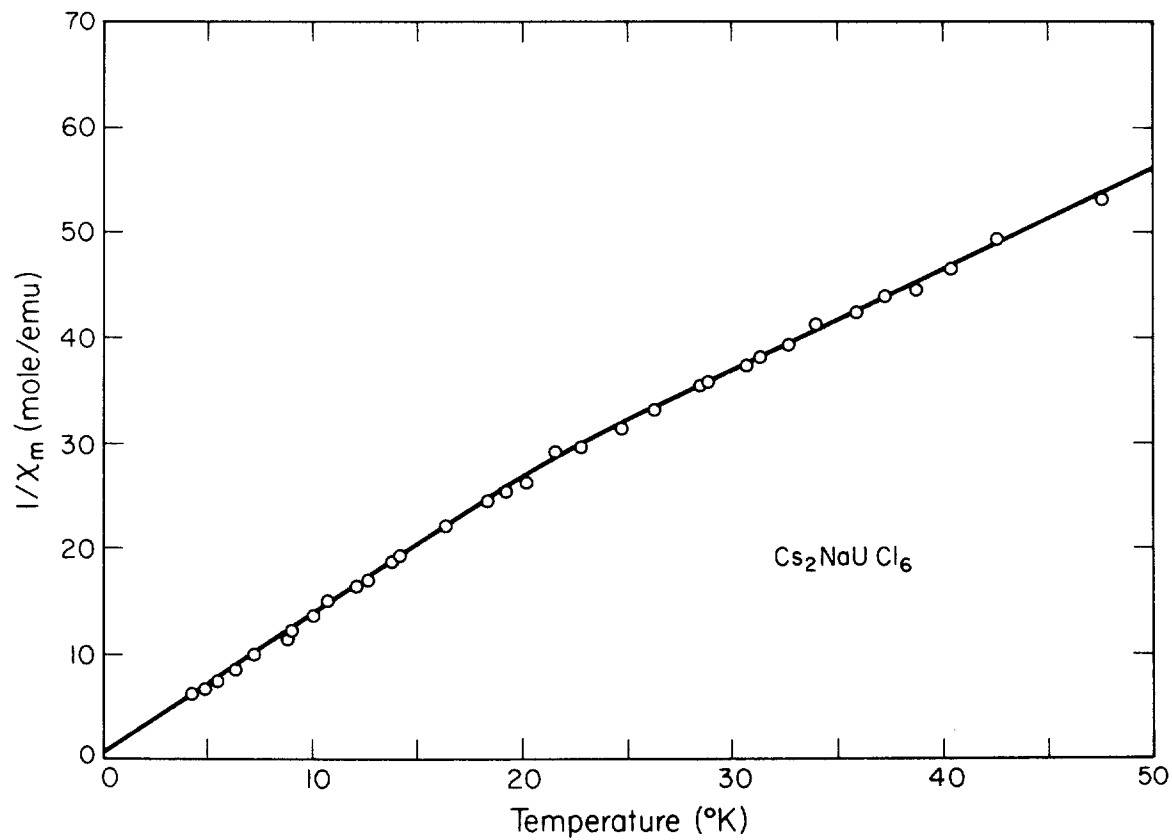


FIGURE 1. Inverse susceptibility of $\text{Cs}_2\text{NaUCl}_6$ below 50°K . The solid line below 20°K gives an effective moment of $2.49 \mu_B$, and above 25°K gives $2.92 \mu_B$.

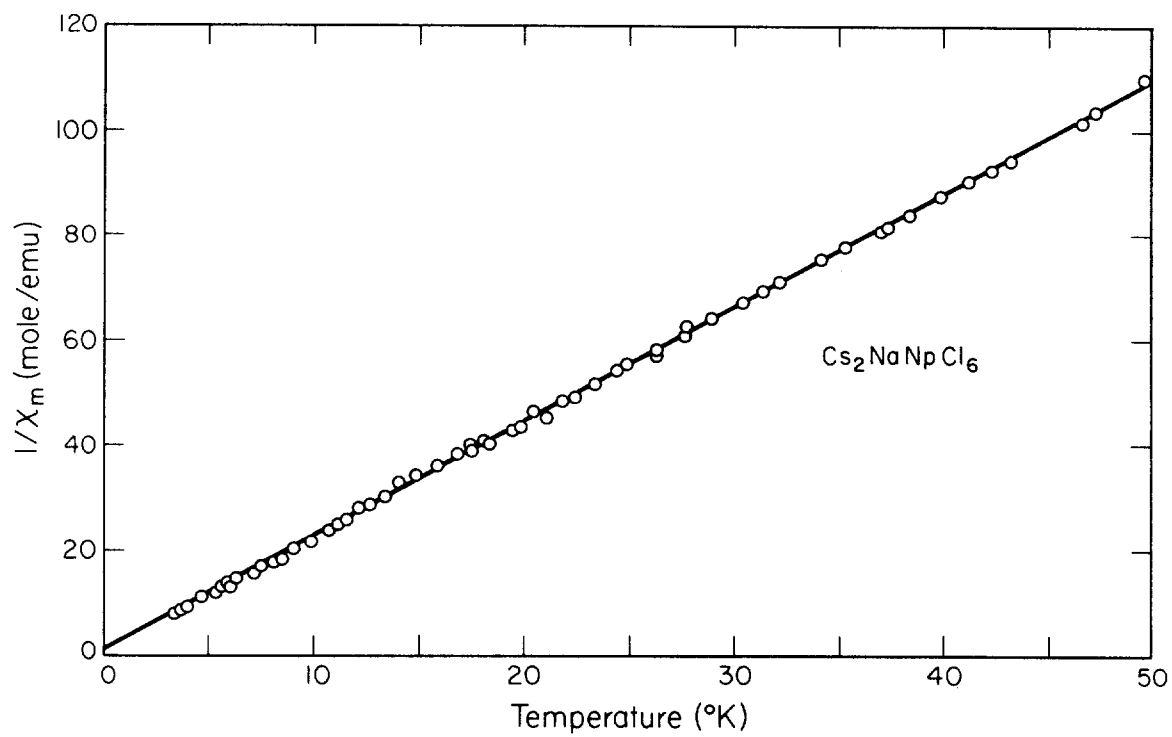


FIGURE 2. Inverse susceptibility of $\text{Cs}_2\text{NaNpCl}_6$ below 50°K . The solid line gives an effective moment of $1.92 \mu_B$.

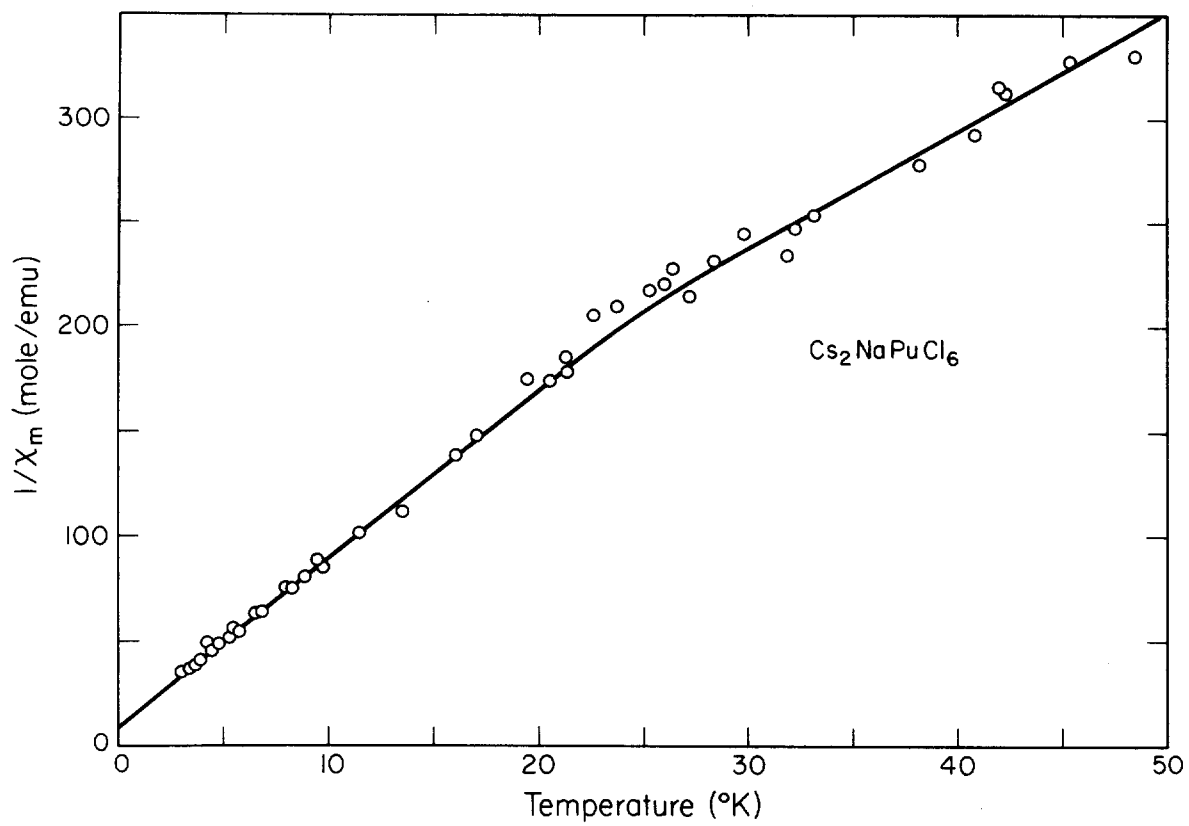


FIGURE 3. Inverse susceptibility of $\text{Cs}_2\text{NaPuCl}_6$ below 50°K . The solid line below 21°K gives an effective moment of $0.97 \mu_B$, and above 25°K gives $1.16 \mu_B$.

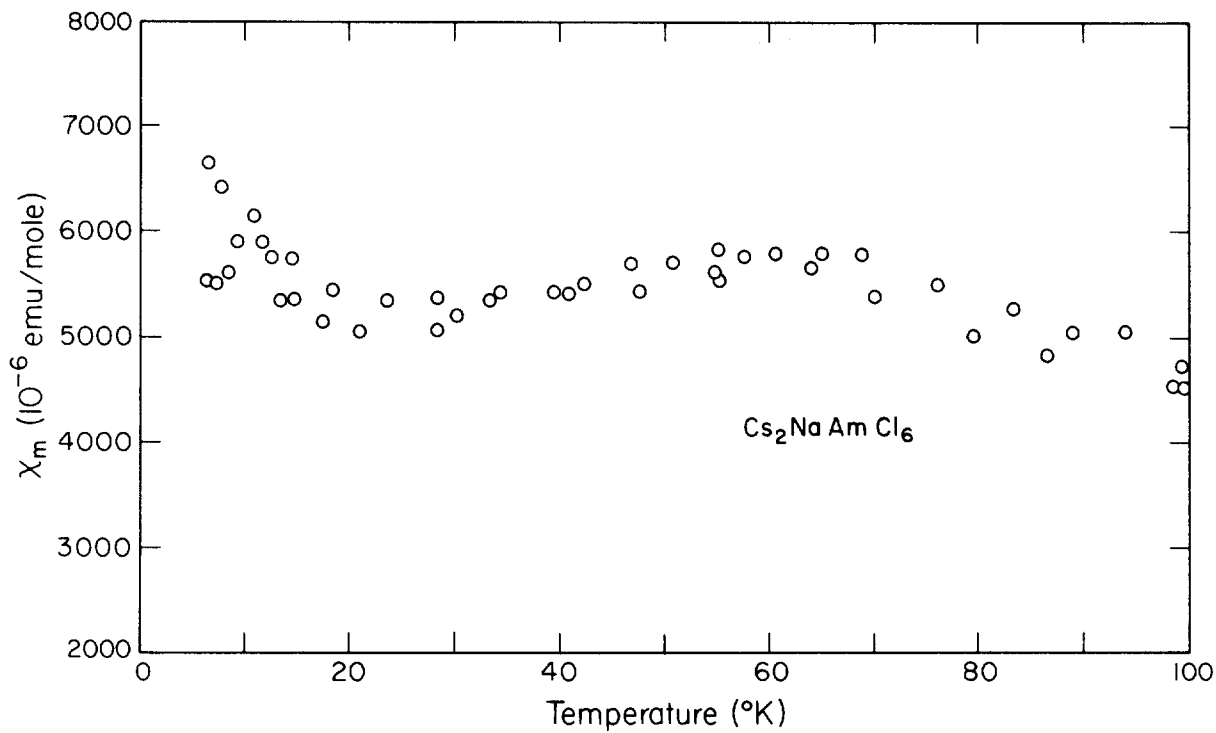


FIGURE 4. Magnetic susceptibility of $\text{Cs}_2\text{NaAmCl}_6$ below 100°K , corrected for Cm^{3+} impurity. Below 70°K the temperature-independent paramagnetic susceptibility is 5400×10^{-6} emu/mole.

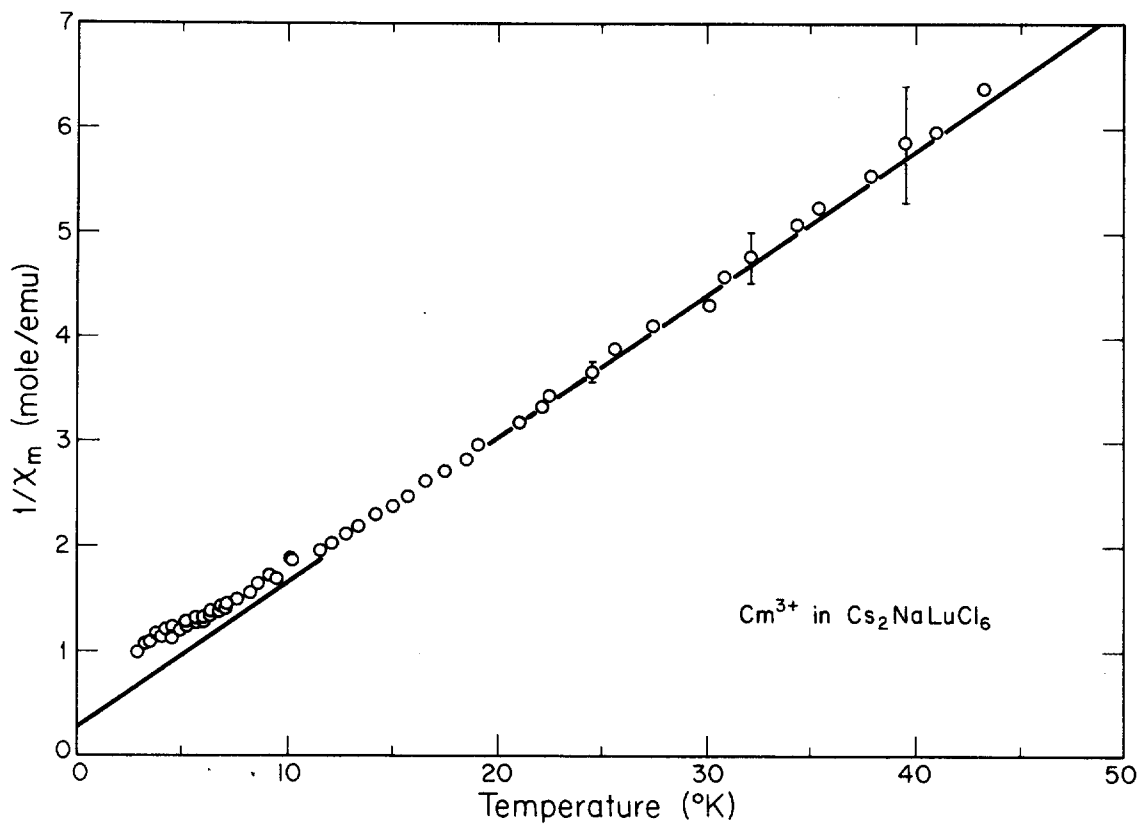


FIGURE 5. Inverse susceptibility of Cm^{3+} in $\text{Cs}_2\text{NaLuCl}_6$ below 50°K . The solid line is for the theoretical free-ion moment, $7.64 \mu_B$; deviations from the free-ion moment at lower temperatures are attributed to crystal-field splitting in Cm^{3+} .

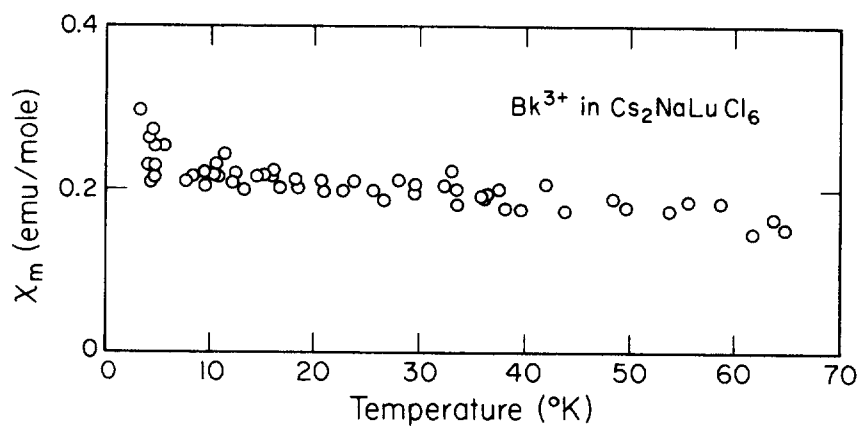


FIGURE 6. Magnetic susceptibility of Bk³⁺ in Cs₂NaLuCl₆ below 70°K. The correction for Cf³⁺ impurity is negligible. Below 40°K the temperature-independent paramagnetic susceptibility is $192\,000 \times 10^{-6}$ emu/mole.

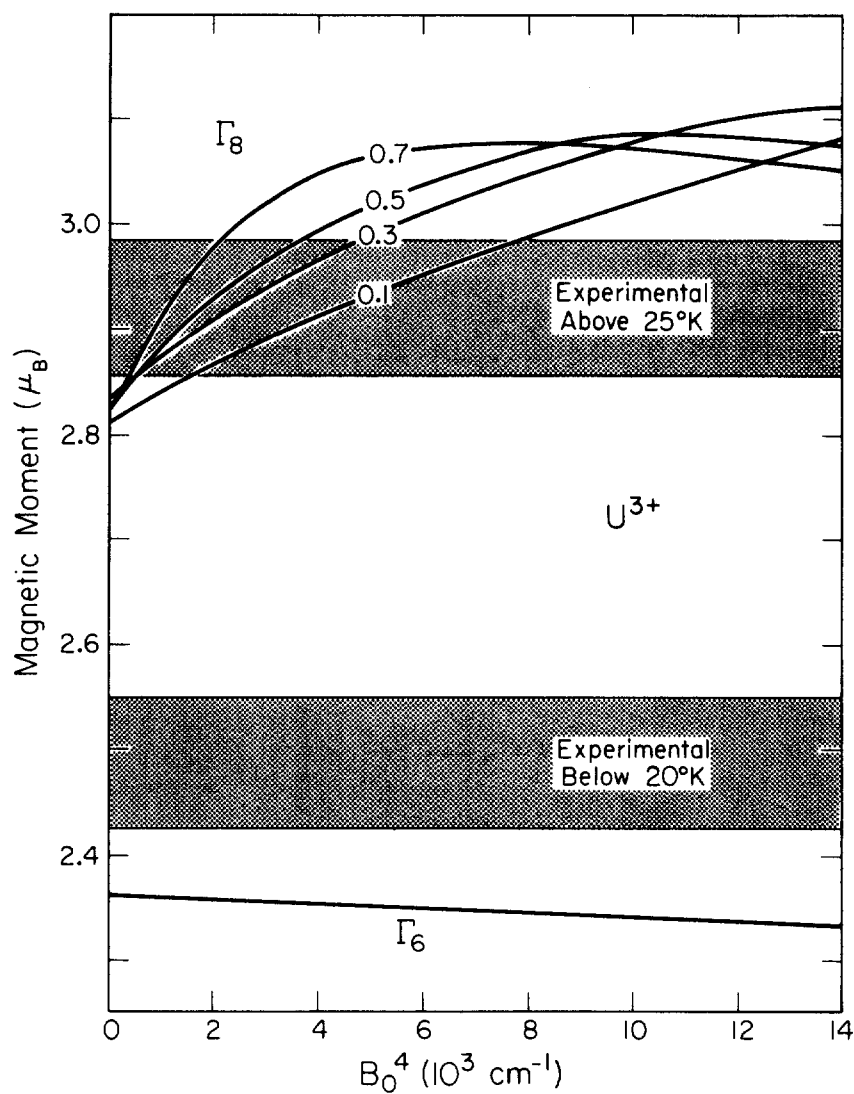


FIGURE 7. Theoretical magnetic moment of the U^{3+} ion in an octahedral crystal field, as a function of the fourth-order crystal-field parameter, B_0^4 . The calculated moments for the Γ_8 level are given for various values of the ratio B_0^6/B_0^4 ; the moments for the Γ_6 level are independent of this ratio. The experimental moments of Cs_2NaUCl_6 in two temperature ranges are shown for comparison.

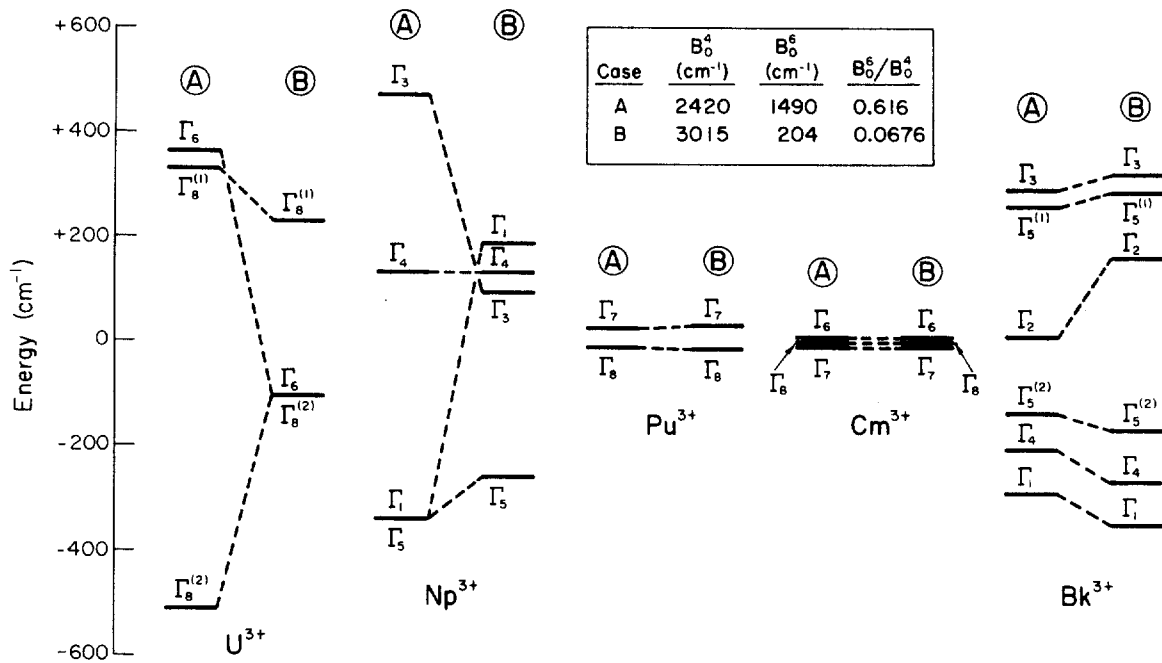


FIGURE 9. Crystal-field splitting of the ground states of trivalent actinide ions in $\text{Cs}_2\text{NaMCl}_6$, calculated for two limiting cases.